Comparison of the dynamic response of a saturated soil between two models

LIN Mian

Institute of Mechanics, Chinese Academy of Sciences, Beijing 100080, China (email: linmian@imech.ac.cn)

Received February 3, 2004

Abstract By comparing the dynamic responses of saturated soil to Biot's and Yamamoto's models, the properties of the two models have be pointed out. First of all, an analysis has been made for energy loss of each model from the basic equations. Then the damping of elastic waves in coarse sand and fine sand with loading frequency and soil's parameters have been calculated and the representation of viscous friction and Coulomb friction in the two models has been concluded. Finally, the variations of loading wave damping and stress phase angles with water depth and soil's parameters have been obtained as loading waves range in ocean waves.

Keywords: models of marine sediment, elastic waves, phase angles of stress field.

DOI: 10.1360/02yd0030

The dynamic response of marine sediment to ocean surface waves is treated extremely by marine geotechnical and coastal engineers. In the area of conventional hydrodynamics, the assumption of impermeable rigid seabed has been used as the boundary of water waves theories and the waves parameters deduced from the theory have not referred to the interaction of water waves and seabed. In the area of soil mechanics, many engineers regard the response as slow loading according to the Zienkewicz's[1] criteria and dynamic analysis is unnecessary. But in the field, some structures have been damaged by the wave-induced seabed instability, rather than their construction causes[2,3]. It is also found that some field measurements and laboratory data do not agree with the static or quasi-static theories[4−6]. Thus, more and more people pay attention to such studies recently[7,8]. Up to now, Biot's model[9] and Yamamoto's model are often used[10]. In this paper, the properties of the two models will be considered for the uses of valid constituting relation in ocean engineering.

1 Comparing the basic equations of two models

Marine sediment is a mixture of three phases: a solid phase (skeletal frame), a liquid phase (pore fluid) and a gas phase (occupying a small portion of pore space). As water waves propagate over a seabed, the pressure gradient induces a flow of pore fluid relative to the skeleton and also causes the skeleton deformation. That is to say, the energy loss of acoustic wave in marine sediment is due to the viscosity friction between fluid and solid and Coulomb friction between grains. So it is a basic problem to study the interaction of them.

Biot's model, assuming a deformable and compressible skeleton for isotropic elastic medium and flow of the compressible pore fluid governed by Darcy's law, is coupled with fluid-grains inertia and viscosity. All of these have basically covered the primary characteristics of soil in static or dynamic situation. The equation of motion of the skeletal frame and pore fluid can be written as

$$\begin{cases} G\nabla^2\boldsymbol{u}+(l+e^2M+G)\nabla e-eM\nabla z \\ \qquad =\dfrac{\partial^2}{\partial t^2}(r\boldsymbol{u}+r_f\boldsymbol{w}), \\ M\nabla(ee-z)=\dfrac{\partial^2}{\partial t^2}(r_f\boldsymbol{u}+m\boldsymbol{w})+\dfrac{h_f}{k_s}\dfrac{\partial \boldsymbol{w}}{\partial t}, \end{cases} \tag{1}$$

where, $r=(1-b)r_r+br_f$ is the bulk density of saturated soil, r_r and r_f are the density of grain and pore fluid, respectively, b is the porosity of the soil; $z=-b\nabla\cdot(\boldsymbol{U}-\boldsymbol{u})$ is the relative dilatability ratio of the fluid, $\boldsymbol{U}$ and $\boldsymbol{u}$ are the displacements of pore fluid and skeleton, respectively; $e=\nabla\cdot\boldsymbol{u}$ is the bulk strain of skeletal frame; $\boldsymbol{w}=b(\boldsymbol{U}-\boldsymbol{u})$ is the fluid displacement relative to skeleton; $e=1-K_s/K_r$ designates the compressibility of soil, K_r and K_s are the bulk modules of grain and skeleton, respectively; $M=K_r^2\big/\left[K_r[1+b(K_r/K_f-1)]-K_s\right]$ designates the compressibility of the pore fluid, K_f is the bulk modulus of the pore fluid; $l=2nG/(1-2n)$ is the Lame's constant, G is shear modulus; h_f and k_s are the coefficient of viscosity of the pore fluid and permeability of the soil, respectively; $m=r_f/b$ is the parameter relating to skeleton.

Obviously, eq. (1) is so cumbersome that some simplified models are often used, such as the quasi-static model[11] for no inertia effects of grain and fluid; the quasi-dynamic model[12] for only the inertia of soil grain or only the compressibility of fluid. In this study, for the sake of understanding the action of the each term and comparing with Yamamoto's model expediently, the original form has been accepted.

Yamamoto first proposed a model for the porous elastic medium to consider the Coulomb friction in the wave-seabed interaction problem. Considering the compressibility of skeleton and pore fluid, the dynamic equation of skeletal frame and pore fluid can be expressed as

$$\begin{cases} \tilde{m}\nabla^2\boldsymbol{u}+(\tilde{H}-\tilde{m})\nabla e-\tilde{C}\nabla z=\dfrac{\partial^2}{\partial t^2}(r\boldsymbol{u}+r_f\boldsymbol{w}), \\ \nabla(\tilde{C}e-\tilde{M}z)=\dfrac{\partial^2}{\partial t^2}(r_f\boldsymbol{u}+m\boldsymbol{w})+\dfrac{h_f}{k_s}\dfrac{\partial \boldsymbol{w}}{\partial t}. \end{cases} \tag{2}$$

The advantage of the model is to consider the weak nonlinear damping induced by the friction of grains and thus the behavior of such material is similar to a visco-elastic material.

For convenience of comparing eq. (1) with eq. (2), the expressions of each parameter are listed in table 1, where $(\Delta w/w)_s$ and $(\Delta w/w)_c$ are the specific loss from cyclic shear and cyclic compression, respectively.

It is found that the mathematical form of the two equations is the same but the physical meanings of the parameters are different. All of $\tilde{H},\tilde{C},\tilde{M},\tilde{m}$ in Yamamoto's model are complex elastic modulus (in this paper, the complex is designated by tildes). These complex moduli imply the energy dissipated per cycle, in which the real part represents the elastic modulus and the image part is the linearized expression of the nonlinear Coulomb damping due to the grain-to-grain friction.

Table 1 Comparing the parameters of two models

Biot's model	Yamamoto's model
Shear modulus G	complex shear modulus $\tilde{m}=G\left(1+i(\Delta w/w)_s/2p\right)$
Bulk modulus for skeleton K_s	complex bulk modulus $\tilde{K}_s=K_s\left(1+i(\Delta w/w)_c/2p\right)$
$C=eM=\dfrac{K_r(K_r-K_s)}{K_r\left[1+b\left(K_r/K_f-1\right)\right]-K_s}$	$\tilde{C}=\dfrac{K_r(K_r-\tilde{K}_s)}{K_r\left[1+b\left(K_r/K_f-1\right)\right]-\tilde{K}_s}$
$H=l+e^2M-2G=\dfrac{(K_r-K_s)^2}{K_r\left[1+b\left(K_r/K_f-1\right)\right]-K_s}+\dfrac{2-2n}{1-2n}G$	$\tilde{H}=\dfrac{(K_r-\tilde{K}_s)^2}{K_r\left[1+b\left(K_r/K_f-1\right)\right]-\tilde{K}_s}+\dfrac{2-2n}{1-2n}G+i\left[G(\Delta w/w)_s+K_s(\Delta w/w)_c\right]/2p$
$m=r_f/b$	$m=(1+a)r_f/b$, a is the added mass of the skeleton

In the early study, many investigators assumed that the energy loss was mainly due to the viscosity frictions[13]. But later some filed measurements[14,15] indicated that there were relative motions between grains except for the motion of fluid-grain. It can be concluded that there are two reasons to cause energy loss: one is due to the viscous friction of fluid-grain and the other due to the solid-to-solid friction at the point of contact between grains. Therefore, we consider that the viscous dissipation is embodied in the Biot's model and damping of viscous friction and that of Coulomb friction are embodied in the Yamamoto's model. In the next section, the properties of the two models will be discussed starting from the elastic waves propagation.

2 Comparison of the damping of elastic waves

There are three types of elastic waves in the porous medium: (i) fast compressional waves induced by the simultaneous motion of pore fluid and skeleton (called *f* wave); (ii) slow compressional waves due to the relative motion of pore fluid to skeleton (called *s* wave); (iii) shear waves represented by the shear vibration (called *T* wave). Assuming loading waves to be harmonic motion $e^{i(wt-\tilde{k}x)}$, the dispersion equation for three elastic waves of Biot's model is derived

$$\begin{cases} \left(HM-C^2\right)\left(\dfrac{\tilde{k}_{f,s}}{w}\right)^4-\left(rM+m'H-2r_fC\right)\left(\dfrac{\tilde{k}_{f,s}}{w}\right)^2+\left(rm'-r_f^2\right) \\ \qquad =0, \\ Gm'\left(\dfrac{\tilde{k}_T}{w}\right)^2-\left(rm'-r_f^2\right)=0, \end{cases} \tag{3}$$

in which $m'=m-ih_f/k_sw$. Similarly, the dispersion equation of Yamamoto's model can be obtained[16] by the substitution of $H\to\tilde{H},C\to\tilde{C},M\to\tilde{M}$, $G\to\tilde{m}$.

Define the damping of the elastic waves as $d_{f,s,T}=8.686w\,\mathrm{Im}(\tilde{k}_{f,s,T}/w)$, where the subscripts *f*, *s*, *T* mean fast compressional waves, slow compressional waves and shear waves, respectively. The calculated parameters are listed in table 2.

2.1 The variations of waves damping with loading frequency

Assuming the value of loading frequency range is from 10^{-2} Hz to 10^4 Hz (fig. 1). In the low frequency range of $10^{-2} < w < 10$ Hz, for the coarse sand (fig. 1(a)) and the fine sand (fig. 1(b)), the damping of *f* waves and that of *s* waves for the two models are almost the same. It implies that both models are analogous for transmit of compressional waves. However, the damping of *T* waves for Yamamoto's model is much larger than that of Biot's. As we know, the mechanism of shear energy dissipation in soil is due to a Coulomb friction, other than viscous friction[14]. Consequently, the Coulomb friction should be considered not only in fine sand seabed but also in coarse sand seabed. Some field measurements have indicated the conclusion[17].

In the high frequency range of $100 < w < 10000$ Hz, for the case of coarse sand (fig. 1(c)), it is clear that the wave damping for Yamamoto's model increases with loading frequency increasing, but for Biot's model, as $w > 1780$ Hz, the damping does not vary with the loading frequency. It is implied that the viscosity frictions stop as the loading frequency reaches some value (Biot's model) and the Coulomb frictions increase with the frequency increasing (Yamamoto's model). The latter is greater than the former. For the case of fine sand (fig. 1(d)), the trend of compressional waves damping is almost the same for the two models. The damping of *T* waves, similar to low

Table 2 Calculated parameters

b	0.4	k_s (m^2)	1.0×10^{-9} (coarse sand), 7.3×10^{-12} (fine sand)
n	0.33	G (N/m^2)	5.0×10^7 (coarse sand), 1.6×10^6 (fine sand)
a	0.25	d	0.05
r_r/kg · m^{-3}	2.65×10^3	K_r	3.6×10^{10}/N · m^{-1}
r_f/kg · m^{-3}	1.0×10^3	K_f	1.92×10^9/N · m^{-1}

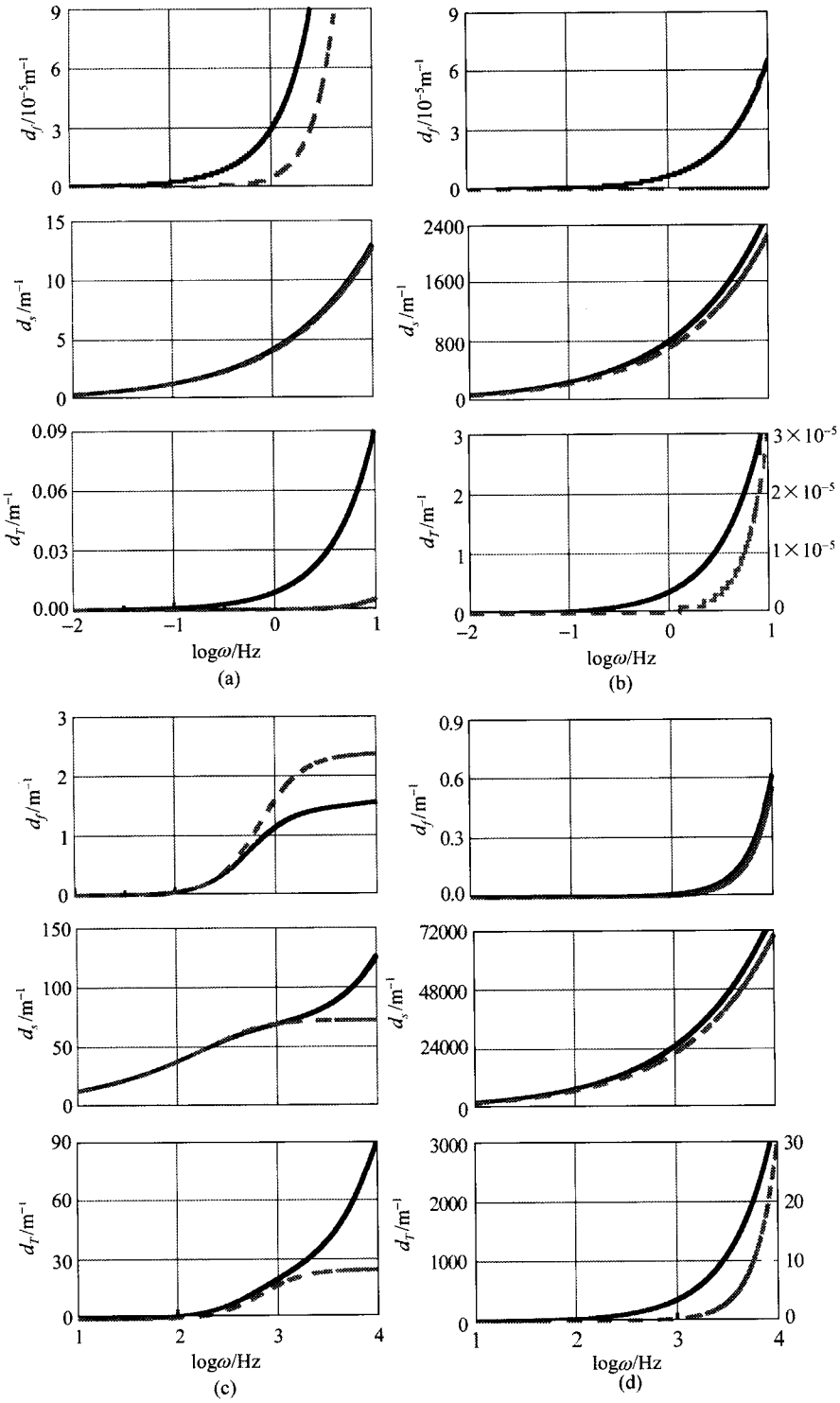

Fig. 1. The variation of elastic waves damping with the frequency of loading waves. The solid line denotes the solution of Yamamoto's model, and the dash line is the solution of Biot' s model.

frequency, for Yamamoto's model, is large and in the order of 10^3 and for Biot's model, is rather small and in the order of 10.

To sum up, for coarse sand, in the range of low frequency, the energy loss is mainly due to the viscous friction and in the high frequency due to the Coulomb friction. Otherwise, it is noticeable that the numerical results of the two models are significantly different though the parameter *d* related to Coulomb friction is rather small. Therefore, the Coulomb friction affects elastic waves within soil distinctly.

2.2 The variations of waves damping with porosity, shear modulus, permeability and viscosity

As seen in fig. 2(a), as the porosity increases, the variations of *f* waves and *T* waves for the two models are quite different. The damping of *f* wave is nonlinear for Biot's model and reaches the maximum at $b = 0.13$, but the damping of *T* waves increases linearly. However, the damping for Yamamoto's model of *f* waves increases monotonously, but *T* waves were reverse. Even so the discrepancy of the energy loss due to shear friction in the two models is much large. Thus, the enlarging porosity could not submerge the effect of Coulomb damping.

Fig. 2(b) shows the damping of compressional waves and shear waves resulting from shear modulus increasing. It is observed that the variations of *f* waves damping for the two models are just reverse. As the shear modulus increases, the damping decreases for Biot's model and the damping increases for Yamamoto's model. The curves reveal that the viscous friction decreases and Coulomb's friction increases when adding an augment stiffness, and the latter is greater than the former. It is also seen from the figure that the damping of *s* waves and *T* waves decreases swiftly in the same way. As $G > 5\times10^7$ N/m^2, the energy loss due to viscose friction and Coulomb friction can be ignored.

Given permeability range from 10^{-10} to 10^{-9} m^2, though the damping of *f* waves and *T* waves increases linearly, the augment is rather small. It can be concluded that the effect of permeability on *f* wave and *T* wave damping is rather small (fig. 2(c)).

The waves damping versus viscosity is plotted in fig. 2(d). As the viscosity enlarges in one order, the damping of *f* waves and *T* waves for Yamamoto's model almost remains, but for Biot's model it nearly approaches zero. It is noticed that the Coulomb damping represented in Yamamoto's model is much larger than viscosity damping and the viscosity damping in Biot's model can be shown in the damping of *s* waves.

Comparing the curves of 12 groups it is found that all the *s* waves damping for Yamamoto's model varying with soil parameters is close to Biot's, and *T* waves damping for Yamamoto's model is three orders larger than that of Biot's at least. It should be concluded that the variations of viscosity friction with soil parameters in the two models are the same and the variations of Coulomb friction with soil parameters have been shown by the curves of *T* wave obtained from Yamamoto's model.

3 Comparing loading waves damping with variations of stress angles

The response of loading wave and stress field within soil are very important to ocean engineering. It is obvious, by comparing the above basic equations, that forms of motion equation of both models are the same, so the relation derived by ref. [16] can be used to calculate the wave damping and the distribution of stress.

3.1 Loading waves damping

Fig. 3 shows the loading wave damping as water wave propagates over coarse sand seabed and fine sand seabed. The damping is almost the same for coarse sand seabed (fig. 3(a)), but for fine sand seabed the damping for Yamamoto model is two orders as great as that of Biot's model (fig. 3(b)), and the results have been proved by the experiment[18], detecting that the motion of seabed makes Coulomb friction strong and enlarges the wave damping. If Coulomb friction has not been taken into consideration even if the seabed motion is considered, the characteristic has not been made clear (Biot's model).

3.2 Comparing stress angles

The angles distributions of pore pressure, shear

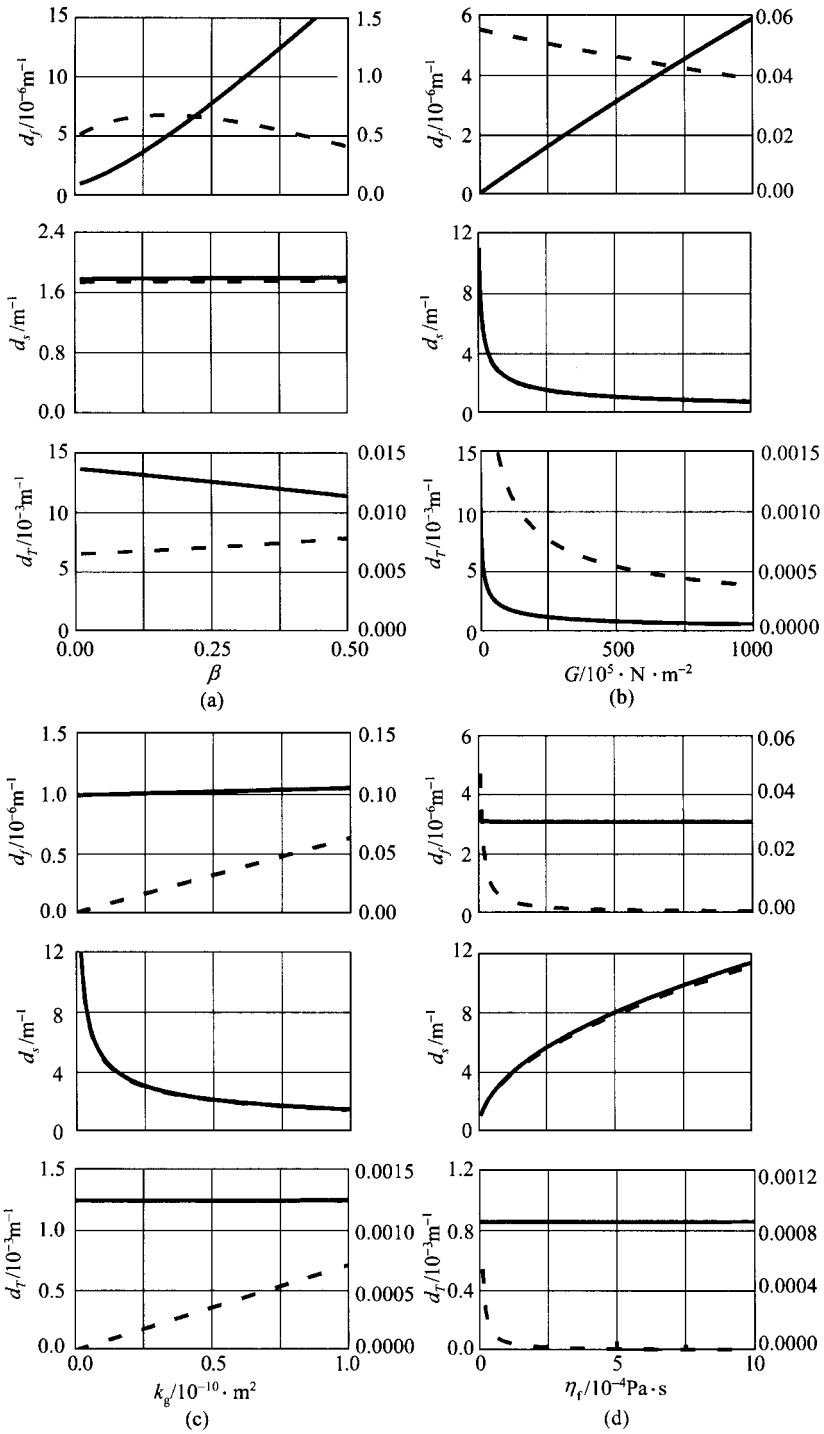

Fig. 2. Elastic waves damping for various soil parameters. The solid line denotes the solution of Yamamoto's model, and the dash line is the solution of Biot's model.

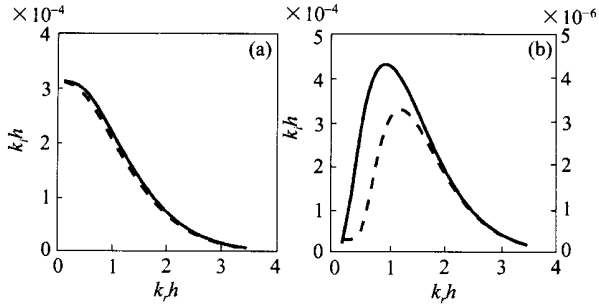

Fig. 3. Loading waves damping in different kinds of sand seabeds, The solid line denotes the solution of Yamamoto's model, and the dash line is the solution of Biot's model.

stress and normal stress plotted in fig. 4(a)—(d) are porosity, shear modulus, permeability and viscosity.

As shown in fig. 4(a)—(c), with the increasing porosity and permeability, the angles of pore pressure are almost identical for the two models and the angles of normal stress and shear stress trend uniformly. Although the tendency of pore pressure angles is reverse for the two models as viscosity varies, the value is rather small, just around 2°. Therefore, we consider that the variations of stress angles with the soil parameters are considerably against the two models. In other words, at that time, the effect of Coulomb friction on stresses field is rather small and could be neglected.

However, more attention should be paid to the distribution of stress angles with shear modulus (fig. 4(d)). As shear modulus $G < 5\times10^5$ N/m^2, the wave-induced pore pressure by Yamamoto's model was out of phase with that of Biot's model extending to 10°. This result exhibits similarity to Sleath's ex-

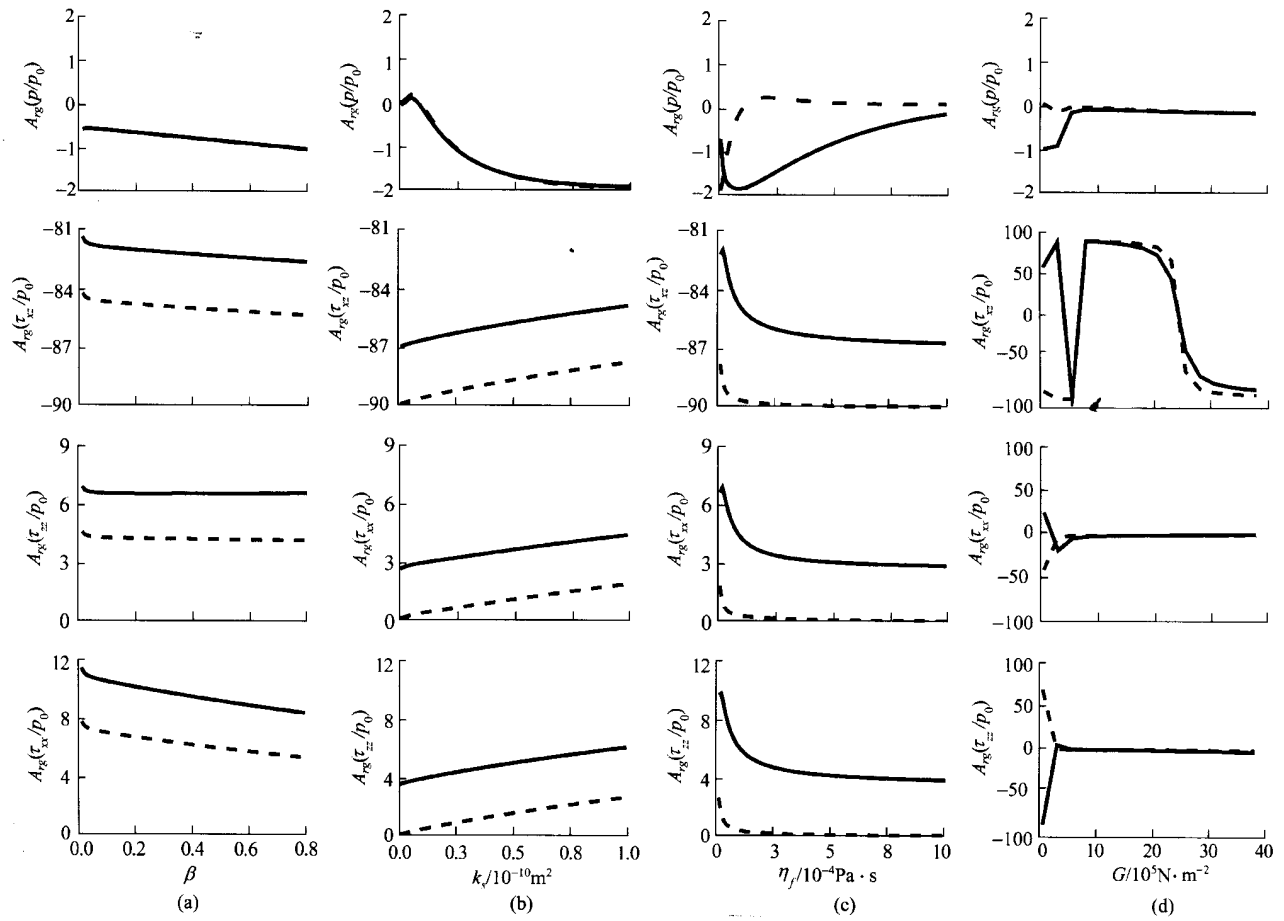

Fig. 4. The variation of stress angles with various values of soil parameters. The solid line denotes the solution of Yamamoto's model, and the dash line is the solution of Biot's model.

periments[19]. At the same time, the angles of normal stress and shear stress for the two models are reverse. As shear modulus $G > 10^6$ N/m^2, both models are almost equivalent. It may be deduced that the stress angles are most sensitive to shear modulus and Yamamoto's model is suitable for the case of $G < 5\times10^5$ N/m^2.

4 Conclusions

The following conclusions can be drawn from the above analysis:

(1) The mechanisms of energy loss embodied in the two models are different, the viscous friction is created by Biot's model and both viscous friction and Coulomb friction are produced by Yamamoto's model.

(2) For low frequency, the viscous frictions play a main part in coarse sand seabed and the Coulomb friction in fine sand seabed. For high frequency, both viscosity friction and Coulomb friction should be taken into consideration in coarse sand seabed and for low frequency, Coulomb friction should be considered in fine sand seabed.

(3) The representations of viscosity friction in the two models correspond with each other, the viscosity friction for Biot's model is reflected on damping of slow compressible waves and the Coulomb friction for Yamamot's model on damping of shear waves.

(4) As shear modulus $G < 5\times10^5$ N/m^2, Yamamoto's model is suitable. As shear modulus $G > 106$ N/m^2, both models are equivalent.

Acknowledgements This work was supported by the National Natural Science Foundation of China (Grant No. 40176027).

References

1. Zienkiewicz, O. C., Bettess, P., Soil and other saturated media under transient, dynamic conditions, in General Formulation and the Validity of Various Simplifying Assumptions, Soil Mechanics-Transient and Cyclic Loads (eds.G.N. Pande, G. N., Zienkiewicz, O. C.), New York: John Wiley & Sons Ltd, 1982, 1—16.
2. Smith, A. W., Gordon, A. D., Large breakwater toe failures, Journal of Waterway, Harbor and Coastal Engineering Division, ASCE, 1983,109 (2): 253—255.
3. Lundgren, H., Lindhardt, J. H. C., Romhild, C. J., Stability of breakwaters on porous foundation, in Proceedings of 12th International Conference Soil Mechanics and Foundation Engineering, 1989, 1: 451—454.
4. Sakai, T., Hatanaka, K., Mase, H., Wave-induced effective stress in seabed and its momentary liquefaction, Journal of Waterway, Port, Coastal and Ocean Engineering, ASCE, 1992, 118(2): 202—206.
5. Zen, K., Yamazaki, H., Field observation and analysis of wave-induced liquefaction in seabed, Soils and Foundations, 1991, 31(4): 161—179.
6. Nye, T., Yamamoto, T., Field test of buried ocean-wave directional spectrometer system, Journal of Waterway, Port, Coastal and Ocean Engineering, ASCE, 1994, 120(5): 451—466.
7. Lee ,T. L., Tsai, C. P., Jeng, D. S., Ocean waves propagating over a Coulomb-damped poroelastic seabed of finite thickness: An analytical solution, Computers and Geotechnics, 2002, 29: 119—149.
8. Jeng, D. S., Lee, T. L., Dynamic response of porous seabed to ocean waves, Computers and Geotechnics, 2001, 28: 99—128.
9. Biot, M. A., Mechanics of deformation and acoustic propagation in porous media, Journal of Applied Physics, 1962, 33: 1482—1498.
10. Yamamoto, T., On the response of a Coulomb-damped poroelastic bed to water waves. Marine Geotechnology, 1983, 5: 93—130.
11. Rahman, M. S., Lee, T. L., Effects of inertia forces on wave-induced seabed response, International Journal of Offshore and Polar Engineering, 1999, 9: 307—313.
12. Jeng, D. S., Rahman, M. S., Effective stresses in a porous seabed of finite thickness: Inertia effects, Canadian Geotechnical Journal, 2000, 37(4): 1383—1392.
13. Dalrymple, R. A., Liu, P. L. F., Waves over soft mud: A two-layer fluid model, Journal of Physical Oceanography, 1978, 8: 1121—1130.
14. Stokoe, K. H. J., Isenhower, W. M., Hsu, J. R., Dynamic properties of offshore silty samples, in Offshore Technology Conference Proceedings, 1980, 2: 289—302.
15. Stoll, D. R., Acoustic waves in ocean sediments, Geophysics, 1977, 42: 715—725.
16. Lin, M., The analysis of silt behaviour induced by water waves, Sci. in China (in Chinese), Ser. E, 2001, 31(1): 86—96.
17. Okusa, S., Nakamura, T., Fukue, M., Measurements of Wave-induced Pore Pressure and Coefficients of Permeability of Submarine Sediments during Reversing Flow (ed. Denness, B.), London: Seabed Mechanics Graham and Trotman Ltd, 1983, 113—122.
18. Yamamoto, T., Experiments and theory of wave-soil interaction, J. Engng. Mech., 1984, 110(1): 95—112.
19. Sleath, J. F. A., Wave-induced pressures in beds of sand, Journal of Hydraulics Division, ASCE, 1970, 96(2): 367—378.